

Digital shearing laser interferometry  
for heterodyne array phasing

J.N. Cederquist, J.R. Fienup, J.C. Marron,  
T.J. Schulz and J.H. Seldin

Environmental Research Institute of Michigan  
P.O. Box 8618, Ann Arbor, Michigan 48107

ABSTRACT

A laser radar using an array of heterodyne detectors offers the possibility of fine resolution angle-angle imaging. The heterodyne measurements, however, are subject to phase errors due to atmospheric turbulence and mechanical misalignment. A method is described that employs digital shearing of the heterodyne measurements as a means to remove phase errors. By this method large phase errors can be corrected without requiring a beacon or a glint. This digital shearing laser interferometry method was investigated theoretically and demonstrated via computer simulations which included photon noise and various types of phase errors. The method was also successfully applied to data collected in a simple laboratory experiment.

1. INTRODUCTION

Laser radars using arrays of heterodyne receivers are being developed. For fine resolution angle-angle imaging, it is necessary to achieve correct phasing of the measurements made by the individual elements of the array of heterodyne receivers. When this is done, a diffraction-limited angle-angle image is formed from the measured data by digital Fourier transformation. The heterodyne measurements, however, are subject to phase errors due to atmospheric turbulence and mechanical misalignment. An important need is for a method by which the measurements can be accurately phased. For this purpose, we have proposed and investigated a new kind of shearing interferometry employing digital shearing [1] that corrects for phase errors by post-processing without the need for a beacon or a glint.

The digital shearing laser interferometry method is theoretically and mathematically developed in Sec. 2. In Sec. 3, the method is demonstrated via computer simulations including the effects of photon noise. A successful laboratory demonstration experiment is described in Sec. 4. A summary is given in Sec. 5.

2. THEORETICAL DEVELOPMENT

Consider a laser which coherently illuminates a distant object. The object scatters, and possibly

Doppler shifts, the laser beam which then propagates to produce an optical field at the receiver. By heterodyning the received optical field with a local oscillator, a complex-valued measurement of the received optical field can be made. Omitting the details of estimating the frequency difference between the object signal and the local oscillator, and of estimating the received optical field from the heterodyne detector signal, we model the measurement,  $G(u, v; t)$ , of the complex-valued received optical field made by an array of receivers at time  $t$  as

$$G(u, v; t) = F(u, v; t) \exp [i\phi_e(u, v)] \quad (1)$$

where  $F(u, v; t)$  is the optical field at the receiver plane scattered from the object and  $\phi_e(u, v)$  is a phase error in the measurement. The phase error may be due to the combined effects of unknown spatially-varying phase shifts in the local oscillator beams, uncertainties in the axial positions of the individual receivers, and atmospheric turbulence. The coordinates  $u$  and  $v$  index over the receiver measurement plane. The optical field,  $F(u, v; t)$ , at the receiver is time-varying owing to the fact that the object will be rotating and/or translating relative to the receiver during the observation time. For objects at long ranges, only a minute rotation is required to produce a new realization of the optical field. It is assumed that many (a few to a few dozen) independent realizations of the optical field will be measured during a short observation time. The phase error  $\phi_e(u, v)$  is assumed to be constant over the observation time.

Laser interferometry by digital shearing operates on the measured data  $G(u, v; t_k)$  taken at times  $t_k$  where  $k$  ranges from 1 to  $K$ . The first step is to form the sum of products of the sheared fields. The result is a quantity  $S_{a0}(u, v)$  which corresponds to a shear distance  $a$  in the  $u$  direction:

$$\begin{aligned} S_{a0}(u, v) &= K^{-1} \sum_{k=1}^K G(u, v; t_k) G^*(u - a, v; t_k) \\ &= \exp[i\phi_e(u, v) - i\phi_e(u - a, v)] K^{-1} \sum_{k=1}^K F(u, v; t_k) F^*(u - a, v; t_k) \quad (2) \end{aligned}$$

and a corresponding quantity  $S_{0b}(u, v)$  with a shear  $b$  in the  $v$  direction. Note that the leading term contains the differences of the phase error in the direction of the shear.

Assuming that the object is diffuse and its reflectivity  $f(x, y; t)$  is delta-correlated, then, for large  $K$ ,

$$K^{-1} \sum_{k=1}^K F(u, v; t_k) F^*(u - a, v; t_k) \simeq F_I(a, 0) \equiv \langle I \rangle \mu(a, 0) \quad (3)$$

where  $F_I(u, v)$  is the Fourier transform of the incoherent object  $f_I(x, y)$  (the object reflectivity for incoherent illumination),  $\langle I \rangle$  is the average intensity at the receiver plane,  $\mu(u, v)$ , the correlation coefficient, is normalized so that  $\mu(0, 0) = 1$  and equality holds as  $K$  approaches infinity. Substituting Eq. (3) into Eq. (2) gives

$$S_{a0}(u, v) \simeq \exp[i\phi_e(u, v) - i\phi_e(u - a, v)] \langle I \rangle \mu(a, 0) \quad (4)$$

and similarly

$$S_{0b}(u, v) \simeq \exp[i\phi_e(u, v) - i\phi_e(u, v - b)] \langle I \rangle \mu(0, b) \quad (5)$$

Thus, in the limit of large  $K$ , the phases of the quantities  $S_{a0}$  and  $S_{0b}$ , which are derived solely from the heterodyne array measurements with phase errors, are the phase differences in two dimensions of the phase error (plus a constant phase term in each dimension due to the phase of  $\mu$ ). The same algorithms as used on conventional shearing or Hartman wavefront sensor data can be used to estimate the phase error from the phase differences. The phase error estimate can be digitally subtracted from the phase of each of the realizations of the measured optical fields, yielding corrected measurements from which diffraction-limited, coherent, speckled images of the object can be computed by Fourier transformation. The coherent images can be noncoherently averaged, i.e., the squared magnitudes of these speckled images can be averaged, to yield an image of the object with reduced speckle contrast, approximating an incoherent image of the object.

By a derivation analogous to that for optical shearing interferometry [2], the standard deviation,  $\sigma_\theta$ , of the phase difference estimates (ignoring photon or other noise) is approximated, for  $|\mu| \sqrt{K} > 10$ , by

$$\sigma_\theta = \sqrt{\frac{1 - |\mu|^2}{2 |\mu|^2 K}} \quad (6)$$

where  $|\mu|$  stands for either  $|\mu(a,0)|$  or  $|\mu(0,b)|$ . Therefore the shear distances  $a$  and  $b$  must be small enough to give a sufficiently large value of  $|\mu|$  (e.g., 0.5). This implies that  $G(u, v; t)$  must be mildly oversampled (less than a factor of 2 over the Nyquist sampling rate) for use in Eq. (2). The constant phases due to the phase of  $\mu$  result in an additional linear phase in each dimension of the phase error estimate. This in turn yields only a shift in the location of the image. If necessary, this shift can be estimated and removed using a low-resolution image of the object.

### 3. COMPUTER SIMULATIONS

Our computer simulation of digital shearing laser interferometry is shown in block diagram form in Fig. 1. The process begins with an incoherent (intensity) reflectivity image of the object to be studied. Complex-valued, coherent object reflectivity realizations are then produced whose real and imaginary parts at pixel  $(x, y)$  are zero mean with a variance equal to one-half the intensity reflectivity at the corresponding pixel. Those coherent object reflectivities are then Fourier transformed and apertured to produce the ideal Fourier data  $F_k(u, v)$ ,  $k = 1$  to  $K$ , where  $K$  is the total number of realizations. [At this point, ideal coherent images can be computed by inverse Fourier transformation, and an ideal noncoherently averaged image can be computed.] The phase error and photon noise are then added to the ideal Fourier data before the digital shearing algorithm is applied as described in Eq. (2). The phase error is then estimated from the phase differences by one of several algorithms. The phase error is subtracted from the degraded Fourier data, corrected coherent images are formed by Fourier transformation and a noncoherently averaged image can be computed.

Figure 2 shows some reference images for the case of high light levels and no phase errors. The incoherent reflectivity of the object used for the computer simulations is shown in part (a). Part (b) shows an ideal incoherent image of the object with diffraction effects included. Part (c) shows an unaberrated coherent image and part (d) shows the effect of noncoherently averaging  $K = 32$  realizations of coherent images to reduce speckle. The image in part (d) is an example of the image quality that a laser radar could be expected to produce for this set of parameters at high received signal levels.

Figure 3 shows the results of applying digital shearing laser interferometry for a quadratic phase error. Part (a) shows, as a reference, the image that would be obtained for no phase error, 3,000 total detected photoelectrons per realization per speckle in the plane containing the heterodyne receiver array, and  $K = 32$  realizations over which to average the speckled coherent images. The local oscillator intensity was modeled as 100 times the average intensity  $\langle I \rangle$  received from the object. This case therefore corresponds to a total of 30 detected photoelectrons per speckle per realization from the object. Part (b) shows the blurred image that would be obtained by noncoherently averaging over 32 images aberrated by a quadratic phase error of about 10 waves peak-to-peak. Some aliasing occurs because of the phase error. Part (c) shows the noncoherently averaged image obtained when the digital shearing laser interferometry phase-error estimate is used to correct the aberration. The successive relaxation method [3] was used to estimate the phase error from the phase error differences given by digital shearing laser interferometry. Part (d) shows the quadratic phase error. It is shown modulo  $2\pi$  with  $-\pi$  black and  $\pi$  white. Part (e) shows the phase error estimate. The offset of the center of the quadratic is a result of the added linear phase term described earlier. The corrected image (c) has been shifted to compensate for the added linear phase. Comparison of images (a) and (c) and

phase errors (d) and (e) shows the high quality of the phase error estimate and resulting imagery. The blurred image (b) with phase error clearly does not resolve the separated triangles but the corrected image (c) does.

Figure 4 shows digital shearing laser interferometry results for the same parameters as Fig. 3, but for a random phase error as shown in part (d). The phase error is uniformly distributed from  $-0.9\pi$  to  $0.9\pi$  and spatially uncorrelated. Each part of Fig. 4 corresponds to the similar part in Fig. 3. Comparison of images (a) and (c) show that the phase error is well-corrected. The linear phase term in the phase error estimate shown in part (e) makes it difficult to compare with part (d). Comparison of Fig. 4(c) with Fig. 3(c) shows that the phase error correction, for the same received signal level, is similar for the random and the quadratic phase error, despite the fact that the blurred image is much worse for the random phase error case as can be seen by comparing Fig. 4(b) with Fig. 3(b).

#### 4. LABORATORY EXPERIMENT

To give greater confidence in the positive computer simulation results, a laboratory experiment was performed. A heterodyne detector array was not available, so a simpler approach which still provides proof of concept was adopted. The experimental setup is shown in Fig. 5. An argon laser illuminated an object consisting of a portion of an Air Force test object, and a reference beam was also brought in. The optical fields from the object and the reference beam interfere at the CCD camera detector array. The return from the reference beam provides the "local oscillator" and the reference beam is sufficiently angularly separated from the object to generate a spatial carrier which allows complete separation of the object from the undiffracted light in the Fourier transform domain of the detector data (i.e., it satisfies the off-axis holography condition). A quadratic phase error is introduced by locating the origin of the expanding reference beam farther from the detector array. 32 realizations were achieved by moving a ground glass in the plane of the object. The aberrated complex-valued Fourier data was arrived at by Fourier transformation of the detected data, extraction of the aberrated image, and inverse transformation.

The results are shown in Fig. 6. Part (a) shows an unblurred coherent image, and part (b) an unblurred averaged image for reference. Part (c) shows a blurred image (extracted from the Fourier transform of the data), and part (d) shows the averaged blurred image. Part (e) shows the estimated phase error, and parts (f) and (g) show a coherent image and the averaged image, respectively, corrected by digital shearing laser interferometry. Note the excellent correction obtained. The predicted phase error was 2.41 waves (vertically) and the estimated phase error was 2.25 waves, peak-to-peak, in reasonably good agreement.

## 5. CONCLUSION

The digital shearing laser interferometry method for correcting phase errors in laser radars using arrays of heterodyne receivers has been successfully demonstrated both in computer simulation experiments including the effect of photon noise and in a simple laboratory experiment including actual detector noise. The method is applicable to images of diffuse objects, requires no glints or beacons, works for both smoothly varying and random phase errors, and gives useful performance at low light levels. The method has a strong potential for use in phasing heterodyne array laser radars and should help to reduce cost, weight, and complexity of heterodyne array systems.

## 6. ACKNOWLEDGMENT

This research was funded by SDIO through NRL under contract N00014-89-K-2014.

## 7. REFERENCES

1. J.R. Fienup, "Phase error correction by shear averaging," Topical Meeting on Signal Recovery and Synthesis III, Technical Digest Series, Vol. 15, Optical Society of America, Washington, D.C., 1989, pp. 134-137.
2. J.W. Goodman, Statistical Optics, Wiley, New York, 1985, Eq. (6.2-41), p. 271. Note that this equation is incorrectly stated in this reference. An additional factor of  $\sqrt{2}$  should appear in the denominator.
3. P. Nisenson, "Speckle imaging with the PAPA detector and the Knox-Thompson algorithm," in Diffraction-Limited Imaging with Very Large Telescopes, D.M. Alloin and J.M. Mariotti, eds., Kluwer, Boston, 1989, pp. 157-169.

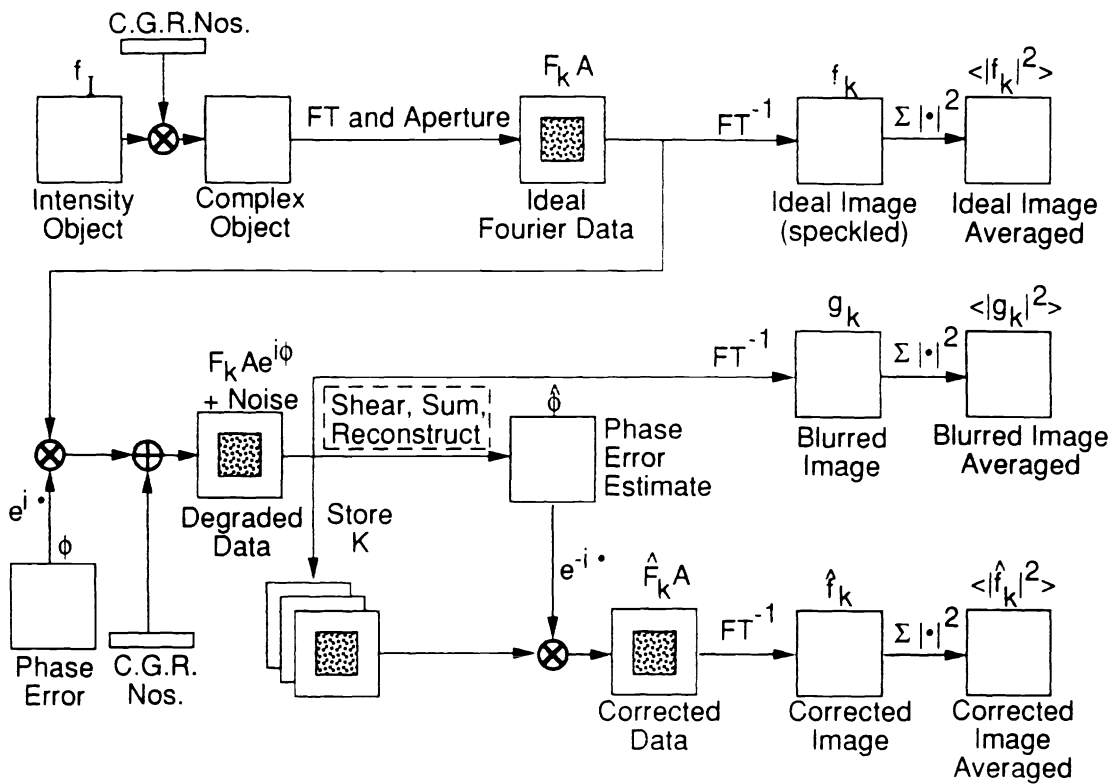


Fig. 1. Block diagram of digital shearing laser interferometry computer simulation.

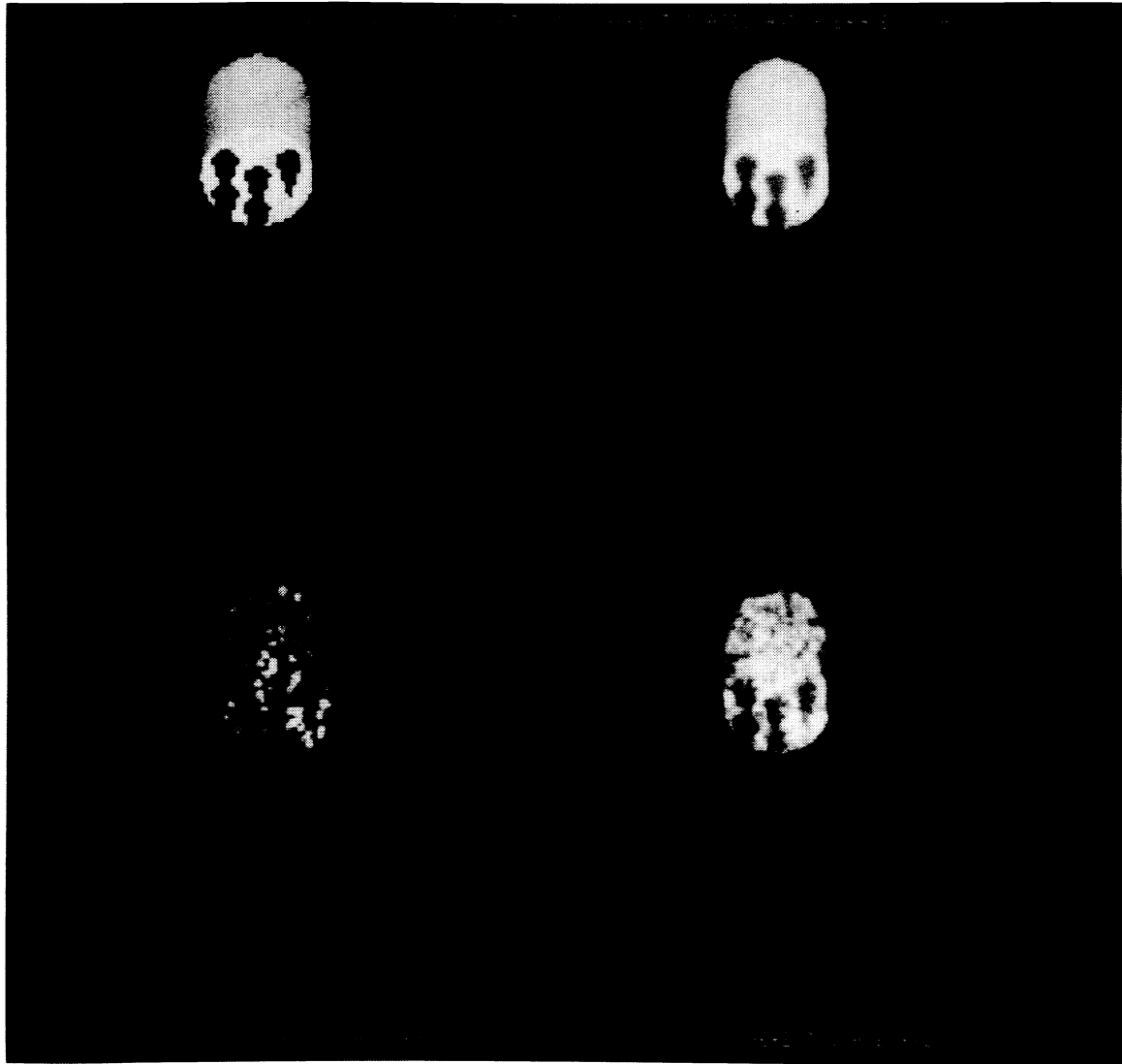


Fig. 2. Reference images. (a) Incoherent object reflectivity, (b) incoherent diffraction-limited image, (c) unaberrated coherent image, and (d) incoherent average of 32 coherent images.

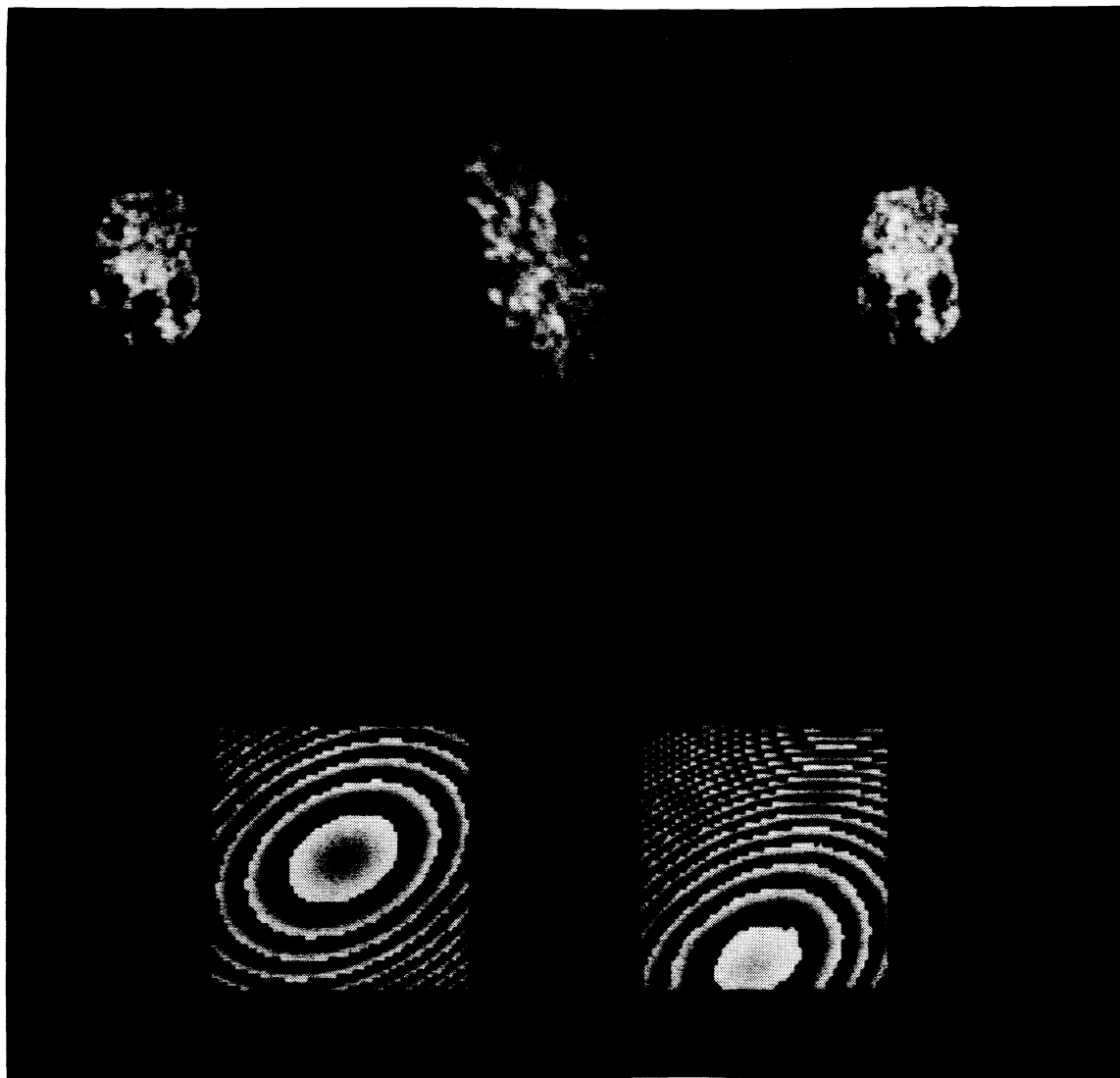


Fig. 3. Phase error correction results for light level of 30 detected object photoelectrons per speckle per realization for quadratic phase error. (a) Reference incoherently averaged image with no phase error, (b) blurred incoherently averaged image with phase error, (c) incoherently averaged image with phase error corrected using laser interferometry, (d) quadratic phase error, and (e) phase error estimated by laser interferometry.

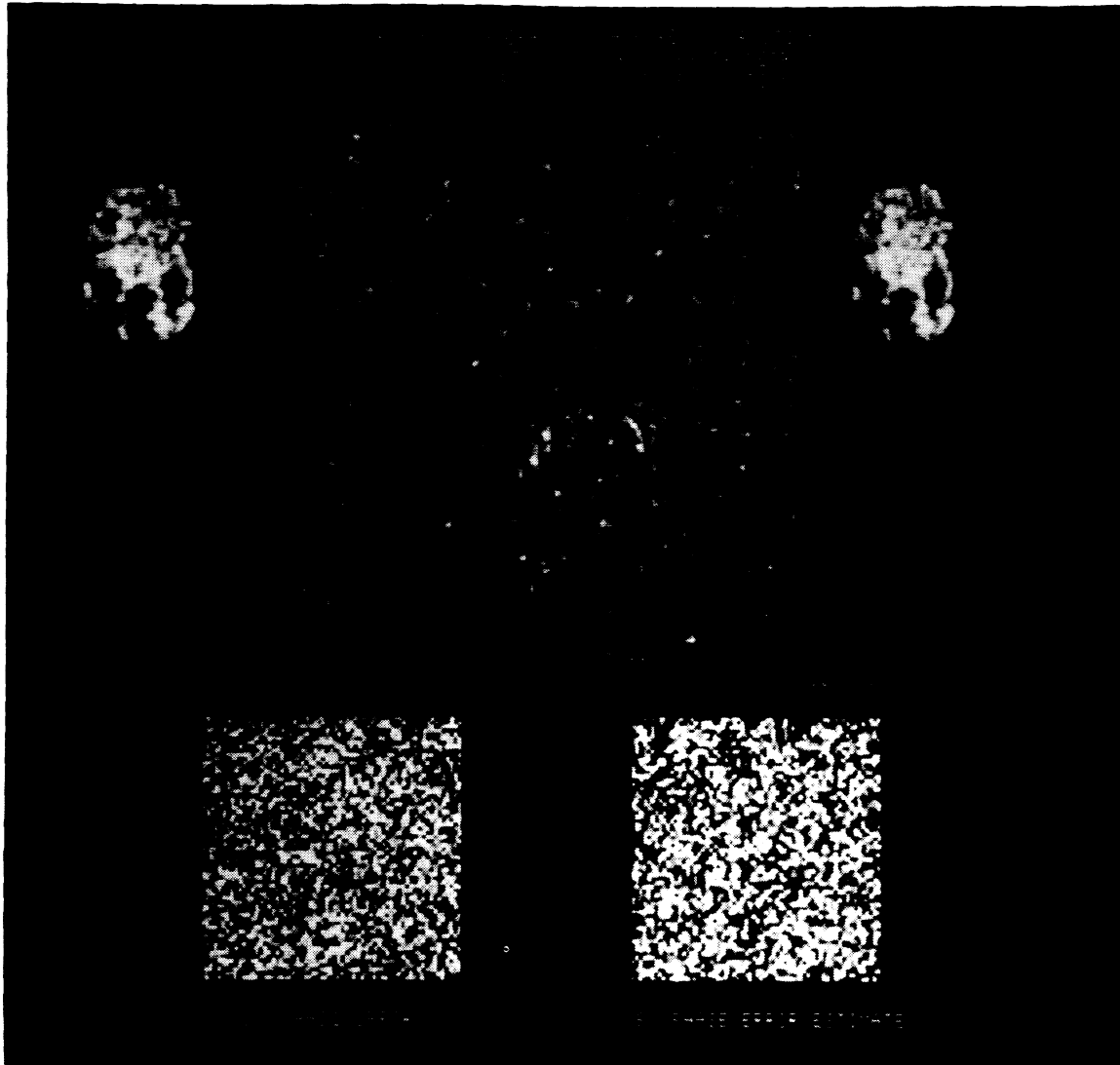


Fig. 4. Phase error correction results for light level of 30 detected object photoelectrons per speckle per realization for random phase error. (a) Reference incoherently averaged image with no phase error, (b) blurred incoherently averaged image with phase error, (c) incoherently averaged image with phase error corrected using laser interferometry, (d) random phase error, and (e) phase error estimated by laser interferometry.

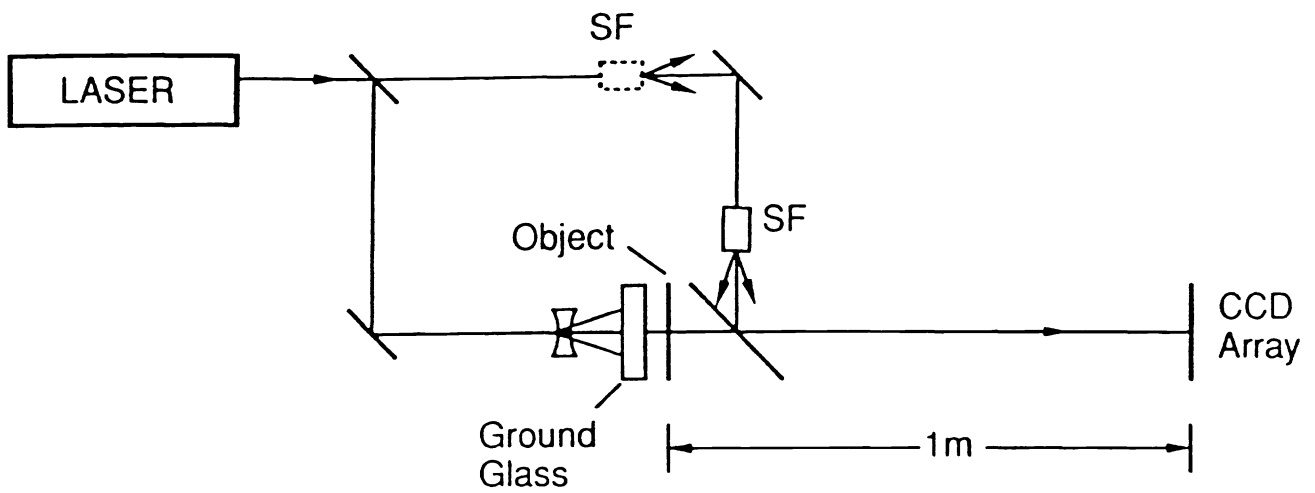


Fig. 5. Laboratory setup for digital shearing laser interferometry proof of concept experiment. SF is spatial filter.

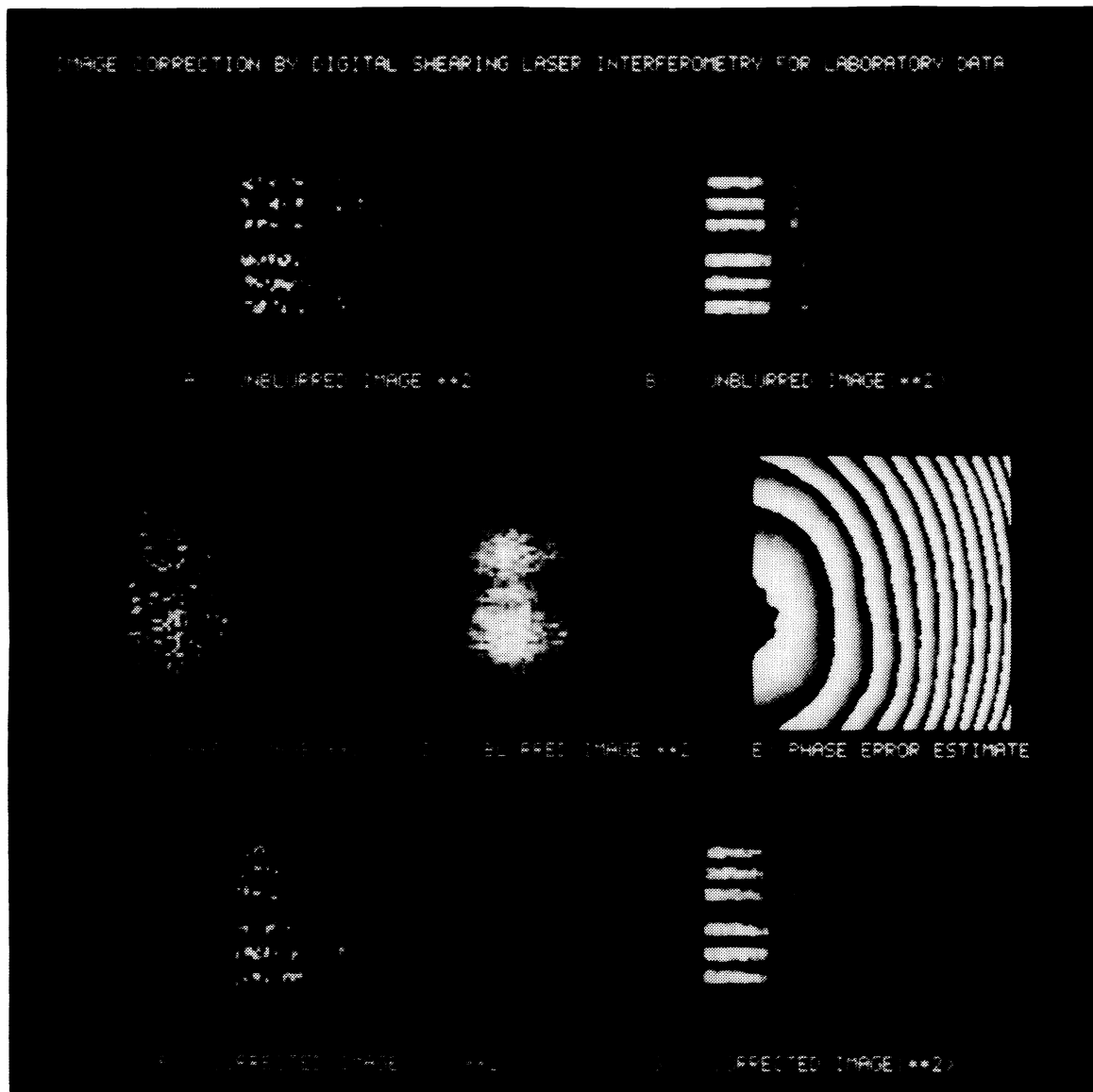


Fig. 6. Experimental phase error correction results. (a) Unblurred coherent image, (b) unblurred incoherently averaged image, (c) blurred coherent image, (d) blurred incoherently averaged image, (e) phase error estimate, (f) coherent image corrected using laser interferometry, and (g) incoherently averaged image corrected using laser interferometry.